Cancer Letters 446 (2019) 112–122

Contents lists available at ScienceDirect

Cancer Letters

journal homepage: www.elsevier.com/locate/canlet

Original Articles

Extracellular adenosine promotes cell migration/invasion of Glioblastoma Stem-like Cells through A_3 Adenosine Receptor activation under hypoxia

Ángelo Torres[a,1], Jose Ignacio Erices[a,1], Fabiola Sanchez[b], Pamela Ehrenfeld[c,d], Laurent Turchi[d,e,f], Thierry Virolle[d,e,f], Daniel Uribe[a], Ignacio Niechi[a], Carlos Spichiger[a], José Dellis Rocha[a], Marcos Ramirez[g,h,i], Flavio Salazar-Onfray[j], Rody San Martín[a], Claudia Quezada[a,*]

[a] Laboratorio de Patología Molecular, Instituto de Bioquímica y Microbiología, Facultad de Ciencias, Universidad Austral de Chile, Valdivia, Chile
[b] Instituto de Inmunología, Universidad Austral de Chile, Valdivia, Chile
[c] Laboratorio de Patología Celular, Instituto de Anatomia, Histología y Patología, Universidad Austral de Chile, Valdivia, Chile
[d] Université Côte d'Azur, Nice, F-06108, France
[e] CNRS, UMR7277, F-06108, France
[f] Inserm, U1091, Nice, F-06108, France
[g] Servicio de Neurocirugía, Instituto de Neurocirugía Dr. Asenjo, Santiago, Chile
[h] Hospital Clínico Universidad de Chile, Santiago, Chile
[i] Instituto Oncológico Fundación Arturo Lopez Perez (FALP), Santiago, Chile
[j] Instituto Milenio de Inmunología e Inmunoterapia, Facultad de Medicina, Universidad de Chile, Santiago, Chile

ARTICLE INFO

Keywords:
A_3 Adenosine Receptor
Ectonucleotidase
Epithelial-Mesenchymal Transition
Prostatic Acid Phosphatase
Hypoxia-Inducible Factors

ABSTRACT

Glioblastoma (GBM) is the brain tumor with the worst prognosis composed of a cell subpopulation called Glioblastoma Stem-like Cells (GSCs) responsible for tumor recurrence mediated by cell invasion. GSCs persist in a hypoxic microenvironment which promotes extracellular adenosine production and activation of the A_3 Adenosine Receptor (A_3AR), therefore, the aim of this study was to determine the role of extracellular adenosine and A_3AR on GSCs invasion under hypoxia. GSCs were obtained from a U87MG cell line and primary cultures of GBM patients, and then incubated under normoxia or hypoxia. Gene expression was evaluated by RNAseq, RT-qPCR, and western blot. Cell migration was measured by spreading and transwell boyden chamber assays; cell invasion was evaluated by Matrigel-coated transwell, *ex vivo* brain slice, and *in vivo* xenograft assays. The contribution of A_3AR on cell migration/invasion was evaluated using the A_3AR antagonist, MRS1220. Extracellular adenosine production was higher under hypoxia than normoxia, mainly by the catalytic action of the prostatic acid phosphatase (PAP), promoting cell migration/invasion in a HIF-2-dependent process. A_3AR blockade decreased cell migration/invasion and the expression of Epithelial-Mesenchymal Transition markers. In conclusion, high levels of extracellular adenosine production enhance cell migration/invasion of GSCs, through HIF-2/PAP-dependent activation of A_3AR under hypoxia.

1. Introduction

Glioblastoma (GBM) is the primary brain tumor with the worst prognosis worldwide [1]. Treatments consist of surgical resection, followed by chemo- and radio-therapy, however patient survival is only 15 months' post treatment [2,3]. This low survival rate is due to the high invasive capacity of GBM, which infiltrates healthy brain tissue, leading to a high relapse rate [2,3]. GBM presents high cellular heterogeneity, highlighting a subpopulation of cells known as Glioblastoma Stem-like Cells (GSCs), responsible for GBM generation and invasiveness [3,4]. In order to invade healthy tissue, cells must detach from the tumor mass, expressing proteins that interact with the Extracellular Matrix (ECM), allowing cell motility [5]. The tumor microenvironment, such as oxygen (O_2) concentration, plays an important role in this process [6]. In brain tissue, O_2 levels range from 2.5 to 12.5%, but in the tumor, these levels decrease drastically to 0.1–2.5% (hypoxia) [7]. The

* Corresponding author. Instituto de Bioquímica y Microbiología, Facultad de Ciencias, Universidad Austral de Chile, Campus Isla Teja s/n, P.O. Box: 567, Valdivia, Chile.
E-mail addresses: claudiaquezada@uach.cl, claudiaquezadaster@gmail.com (C. Quezada).
[1] Co-first authors.

https://doi.org/10.1016/j.canlet.2019.01.004
Received 2 June 2018; Received in revised form 27 December 2018; Accepted 10 January 2019

Nonstandard abbreviations

$A_{2B}AR$	A_{2B} Adenosine Receptor
A_3AR	A_3 Adenosine Receptor
ACTB	Actin-beta
aCSF	artificial Cerebro-Spinal Fluid
DAVID	Database for Annotation, Visualization and Integrated Discovery
EMT	Epithelial-Mesenchymal Transition
ECM	Extracellular Matrix
ERK	Extracellular signal–Regulated Kinases
FBS	Fetal bovine serum
GEO	Gene Expression Omnibus
GBM	Glioblastoma
GSCs	Glioblastoma Stem-like Cells
HPLC	High-performance liquid chromatography
HIF	Hypoxia-Inducible Factor
ICC	Immunocytochemistry
ICF	Immunocytofluorescence
MMP-9	Matrix Metallopeptidase 9
MIF	Migration inhibitory factor
PFA	Paraformaldehyde
PI3K	Phosphatidylinositol-4,5-bisphosphate 3-kinase
p-FAK	phospho-Focal Adhesion Kinase
PC	Primary Cultures
PAP	Prostatic Acid Phosphatase
RQN	RNA Quality Number
siRNA	Small interfering RNA
SD	Standard Deviation

presence of hypoxic niches is associated with a poor prognosis, because the low concentration of O_2 in the tumor microenvironment favors invasiveness [8]. Under this hypoxic microenvironment, GBM cells can adapt due to the expression of Hypoxia-Inducible Factors 1 and 2 (HIF-1 and HIF-2) [7], which promote tumor progression through the induction of genes associated with cellular invasion [9]. Additionally, this hypoxic microenvironment promotes maintenance of the stem phenotype of GSCs, favoring a more aggressive GBM [7,10]. Association of the hypoxic microenvironment with tumor invasiveness in GBM has already been reported, especially in the GSCs subpopulation [11]. Under both normoxia and hypoxia conditions, silencing of HIF-1α expression in GBM cells decreases cell migration *in vitro*, and decreases cell invasion to cerebral parenchyma *in vivo* [12]. Additionally, under hypoxia the expression of transcription factors such as TWIST and SNAIL favors invasiveness by activating Epithelial-Mesenchymal Transition (EMT) [13,14]. Another important aspect in the hypoxic microenvironment is the increased extracellular production of adenosine [15], which is involved in the regulation of several tumorigenic characteristics in GBM [7,16–18]. Under physiological conditions, extracellular adenosine levels oscillate in concentrations between 30 and 200 nM; however, during inflammation, hypoxia, or tumor formation, an increase of up to 100 times its normal concentration occurs [7]. Extracellular adenosine produced in the GBM microenvironment is mainly a result of the action of two ectoenzymes; Ecto-5′-nucleotidase (CD73) [16,18] and Prostatic Acid Phosphatase (PAP) [19], which hydrolyze extracellular AMP to adenosine modulating several cellular processes through purinergic P1 receptors; however, under hypoxia, adenosine levels increase activating low-affinity Adenosine Receptors as A_3 (A_3AR). Interestingly, CD73 enhances cell adhesion through adenosine production, thereby promoting cell migration and invasion [20–23]. Another group demonstrated that extracellular adenosine derived from CD73 activity increases invasiveness of breast cancer cells *in vivo* [24]. In addition, adenosine signals can modulate the EMT in certain types of neoplasms such as head and neck cancer and gallbladder cancer, resulting in a more invasive phenotype [21]. The role of extracellular adenosine as a regulator of the invasive phenotype in GBM cells has been previously demonstrated, where inhibition of CD73 activity and pharmacological blockade of adenosine receptors decreased adhesion to the ECM in the human GBM cell line, U138MG [25]. All together, these previous observations demonstrate a relationship between adenosine signaling and cell migration/invasion in GBM, although, the role of extracellular adenosine and A_3AR on the invasive capacity of GSCs have not yet been evaluated. Previously, our group has shown that GBM-derived cells have a higher production of extracellular adenosine, and that this production is higher in GSCs than in non-GSCs [18]. Additionally, increased adenosine under hypoxia promotes tumorigenic characteristics of GSCs [26,27]. This study focused on the relationship between the migratory/invasive capacity of GSCs and the extracellular adenosine axis under hypoxia, to understand how extracellular adenosine regulates this aspect in GSCs through A_3AR activation.

2. Materials and methods

2.1. Pharmacological agents

For *in vitro* studies MRS1220 (10 μM; Tocris®) was used as a selective A_3AR antagonist [18] and 0.001% DMSO as a vehicle during 24 h. For *ex vivo* studies MRS1220 (10 μM; Tocris®) was refreshed every 3 days during 21 days. For *in vivo* studies we used MRS1220 at 0.15 mg/kg/72 h (intraperitoneal) [18] in NOD/SCID-IL2Rγ^{null} mouse during 10 days. AOPCP (50 μM; α,β-Methyleneadenosine 5′-diphosphate) was used *in vitro* as a CD73 inhibitor (M8386; Sigma, Saint Louis, MO) [16,18] during 24 h.

2.2. GBM samples and primary culture

Tissue samples were obtained by surgical resection procedures of GBM patients at the Departamento de Neurocirugía, Instituto de Neurocirugía Asenjo, Santiago, Chile. All procedures were carried out with the approval of the Bioethics Committee of the Universidad Austral de Chile (Permit Number: 29–2011) and Servicio de Salud Metropolitano Oriente. Tissues were washed twice with HBSS and digested with type I collagenase (3 mg/mL; Gibco®) at 37 °C for 30 min. The reaction was stopped by using DMEM-F12-10% fetal bovine serum (FBS), then filtered through a nylon mesh with 70 μm pores (CLS431751; Sigma, Saint Louis, MO) and centrifuged at 700 × *g* for 5 min. Sediment was cultured in DMEM-F12-10% FBS at 37 °C with 5% CO_2 atmosphere. Finally, Primary Culture (PC) of two different GBM patients were generated and named PC1 and PC2 respectively.

2.3. Glioblastoma Stem-like Cell culture and hypoxia

To generate GSCs, PC (PC1 and PC2), and U87MG (ATCC® HTB-14™) cells were grown at 37 °C in neurobasal medium (Gibco®) supplemented with EGF (20 ng/mL; PeproTech ©), bFGF (20 ng/mL; PeproTech ©), 1× B27 (w/o vitamin A; Gibco®), penicillin/streptomycin (100 units/mL; Gibco®), and L-glutamine (2 mM; Gibco®) [18]. The medium was changed every 3 days, and after 7 days of culture GSCs were characterized (Fig. S1) and plated to carry out different tests. Normoxia (21% O_2) and hypoxia (0.5% O_2) conditions were generated using a gas mixing chamber (5% CO_2 and 95% N_2 mixture) during 24 h.

2.4. Immunocytofluorescence

GSCs were seeded in a pre-treated Poly-L-Lysine coverslip, washed

with 0.1 M phosphate buffer (pH 7.4), and fixed (3.7% PFA) for 10 min [18]. Cells were blocked using 2.5% normal horse serum blocking solution (S-2012, Vector laboratories) for 45 min. Samples were incubated overnight with primary antibodies (Table S1) at 4 °C, then with the secondary antibody Alexa-488 (Table S1) for 1 h and DAPI (300 nM; Thermo Fisher Scientific) for 2 min as a nuclei counterstaining (Fig. S1B). Finally, cells were mounted (S3023; Agilent Technologies, Inc.) and visualized using an epi-fluorescence and light microscopes (Zeiss).

2.5. Adenosine quantification

U87MG- and PC- GSCs were cultured under normoxia and hypoxia during 24 h. Then GSCs were incubated in 1 mL of Tyrode's buffer for 1 h at 37 °C and 200 µL of this incubation medium was mixed with 100 µL of citrate buffer (pH 4). Adenosine was quantified by HPLC fractionation in a Chromolith Performance RP-18e column (Merck) and by fluorescent detection using 2-chloroacetaldehyde derivatizations protocol [18]. Adenosine concentrations (nM) were normalized to the total protein levels (µg).

2.6. RNA extraction and RT-qPCR

GSCs of the U87MG cell line and PC were cultured under normoxia and hypoxia for 24 h. Then total RNA was extracted by TRIzol Reagent (Thermo Fisher Scientific) and reverse transcription was performed with 1 µg of RNA using the M-MLV Reverse Transcriptase (Thermo Fisher Scientific). qPCR assay was performed using the ΔΔCt method and ACTB as a normalizer gene [18]. qPCR reaction was performed with 250 nM of each primer (Table S2) using the 5× HOT FIREPol® EvaGreen® qPCR Mix Plus (ROX) (Solis BioDyne, Tartu, Estonia) following the manufacturer's instructions.

2.7. Western blots

Proteins (50 µg) of U87MG- and PC- GSCs were separated by SDS-PAGE, transferred to 0.22 µm PVDF membranes and blocked with 1× PBS/0.05%tween/1%BSA or 5% non-fat milk for 1 h. Then membranes were incubated overnight with primary antibodies (Table S1) at 4 °C followed by a secondary antibody-HRP conjugate during 1 h. Bands were visualized using the SuperSignal™ West Dura Extended Duration Substrate kit (Thermo Fisher Scientific) and images were quantified by densitometry analysis (ImageJ, NIH).

2.8. siRNA transfection

Commercial siRNAs (all from Santa Cruz Biotechnologies) of ecto-nucleotidases [CD73 (sc-42862) and PAP (sc-72131)], HIFs [HIF-1α (sc-45919) and HIF-2α (sc-35316)] and scramble (sc-37007) were tested *in vitro*. GSCs were cultured in a 6-well plate (2×10^5 cells/well) and then transfected for 6 h with 1 µg of siRNA per well using a Lipofectamine 2000 (Thermo Fisher Scientific) kit following the manufacturer's instructions. 48 h post-transfection GSCs were plated to carry out different tests under normoxia and hypoxia conditions.

2.9. Cell adhesion assay

Pre-treated GSCs were seeded in a 96-well plate (2×10^4 cells/well) and incubated at 37 °C for 2 h in neurobasal medium plus 1% FBS to trigger cell adhesion [25]. Non-adherent GSCs were carefully removed by inverting the culture plate and adherent GSCs were fixed (PFA 3.7% for 10 min) and stained (0.5% crystal violet/20% methanol for 10 min). GSCs were washed with 1× PBS and incubated with 10% acetic acid (v/v) for 5 min. Cell adhesion was analyzed by measuring the optical density of the eluted crystal violet stain at 570 nm in a microplate reader (Synergy 2 Biotek).

2.10. Cell spreading assay

Cell spreading was evaluated using an adapted protocol described by Dasari *et al.*, [28]. Briefly, 2×10^4 U87MG-GSCs were incubated per well in a pre-coated Poly-L-Lysine 6-well plate in 1% fetal bovine serum (FBS) neurobasal medium during 24 h under different conditions. The number of cells outside the neurosphere core was counted and normalized to 1 using the basal condition (siRNA-scramble or vehicle) under normoxia as a calibrator.

2.11. Cell migration assay

24-well plates with 8.0 µm pore transwell inserts (Corning®) were used for cell migration assay [9,14]. The bottom of transwell inserts were coated overnight with 15 µg/mL of bovine fibronectin. A total of 1×10^5 GSCs were seeded into the top of transwell and in the bottom of the well 650 µL of neurobasal medium 10% FBS was used as a chemoattractant during 24 h under different conditions. Cells in the bottom of the well were fixed with 70% ethanol for 10 min and stained using 0.1% crystal violet during 10 min. Cells were counted using the 10× objective in 5 different quadrants.

2.12. Cell invasion assay

24-well plates (6.5 mm, 8.0 µm pore Polycarbonate membrane; Corning®) with matrigel-coated transwell inserts were used [14]. 5×10^4 GSCs were seeded into the top of the matrigel. In the bottom of the well, 650 µL of neurobasal medium 10% FBS was used as a chemoattractant during 24 h under different conditions. Cells in the bottom of the well were fixed (3.7% PFA) and stained (0.1% crystal violet) during 10 min. Cells were counted using the 10× objective in 5 different quadrants.

2.13. Organotypic brain slices and ex vivo cell invasion assay

Organotypic brain slices from the telencephalon portion were generated following the method described by Kim *et al.*, [29] with slight modifications. Brains from 2-month-old mice were removed and collected in chilled artificial Cerebro-Spinal Fluid (aCSF) (124 mM NaCl, 3 mM KCl, 26 mM $NaHCO_3$, 2 mM $CaCl_2$—$2H_2O$,1 mM $MgSO_4/7H_2O$, 1.25 KH_2PO_4, 10 mM D-Glucose) previously oxygenated (95% O_2–5% CO_2 gas) and kept on ice. Then, brains were washed in freshly chilled aCSF and immersed in 4% low-melting point agarose at 37 °C. Coronal brain slices of 300 µm were generated using a vibratome (Leica VT1000 S), and positioned in a membrane insert (0.4 µm pore and 30 mm diameter; Merck) on a 6-well plate. 2×10^5 GSCs were seeded over the brain slice and cultured at standard conditions. On the bottom, 1.5 mL of neurobasal medium 10% FBS was used as a chemoattractant. Finally, GSCs were treated during 21 days with MRS1220 (10 µM; Tocris®) or vehicle (0.001% DMSO), changing the medium every 3 days. To evaluate *ex vivo* cell invasion, brain slices were paraffin embedded and serial sections of 5 µm were mounted on silanized slides. For immunodetection of human GSCs in mice brain slices, samples were dewaxed and hydrated using alcohols in decreasing concentration, immersed in citrate buffer (pH 6) and heated until boiling. Preparations were blocked (5% BSA for 45 min and 2.5% normal horse serum for 45 min), and incubated with anti-human Vimentin antibody overnight at 4 °C. A secondary antibody, Alexa-488, was used, and DAPI (300 nM; Thermo Fisher Scientific) was used as a counterstain. Cells were visualized using an epi-fluorescence microscope (Zeiss).

2.14. In vivo glioblastoma subcutaneous tumors

All animal studies were approved by Bioethics Committee of the Universidad Austral de Chile (Permit Number: 29–2011) according to the NIH Guide for the Care and Use of Laboratory Animals. NOD/SCID-

IL2Rγ^{null} mice (No.005557; The Jackson Laboratory©, USA) were maintained under standard laboratory conditions (12 h light-dark cycle) with food and water ad libitum. 10,000 human U87MG GSCs were inoculated by subcutaneous injection at the left flank of mice previously anesthetized [ketamine (100 mg/kg)/xylazine (10 mg/kg) intraperitoneal]. One week post-inoculation, mice were treated with vehicle (DMEM:F12–0.001% DMSO) and MRS1220 (0.05 mg/kg/day) during 10 days [18]. Animals were euthanized (Sodium Thiopental; 120 mg/kg/intravenous), subcutaneous tumors were removed and fixed in 3.7% paraformaldehyde (Sigma-Aldrich, Germany) for histopathological analysis.

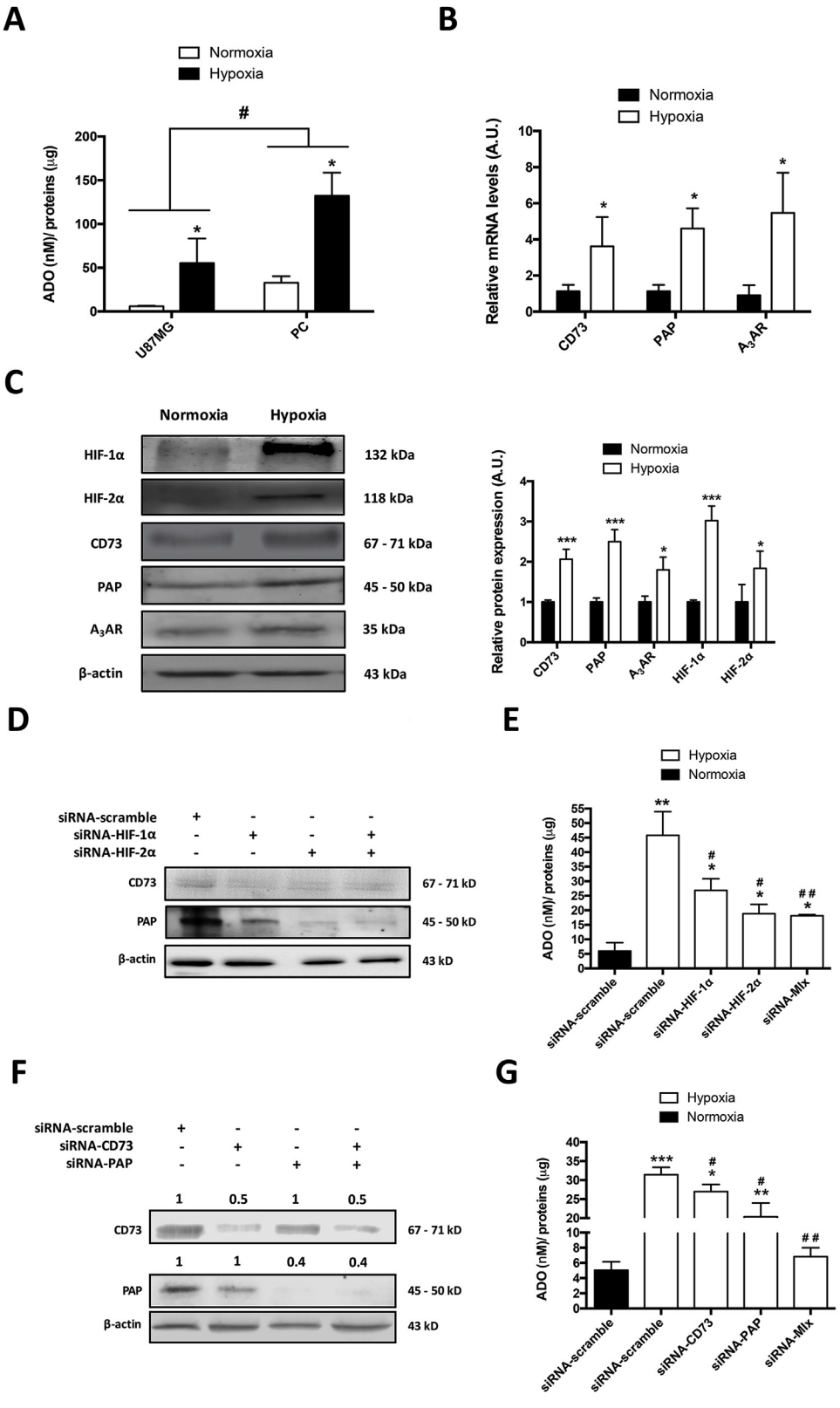

Fig. 1. Extracellular adenosine metabolism in Glioblastoma Stem-like Cells under hypoxia. **(A)** Extracellular adenosine accumulation (nM) measured by HPLC in GSCs of the U87MG cell line and PC cultured under normoxia and hypoxia for 24 h. **(B)** RT-qPCR of CD73, PAP, and A_3AR in PC-GSCs under normoxia and hypoxia for 24 h. Values were normalized to ACTB mRNA expression. **(C)** Representative western blot (left panel) and quantifications (right panel) of HIF-1α, HIF-2α, CD73, PAP, A_3AR, and β-actin in U87MG-GSCs under normoxia and hypoxia for 24 h. The normoxia condition was normalized to 1 (A.U. = Arbitrary Units) and used as a calibrator in B and C. **(D)** Representative western blots of CD73, PAP, and β-actin in U87MG-GSCs knock down (siRNA) for HIF-1α, HIF-2α, and HIF-1α/2α (siRNA-Mix) under hypoxia for 24 h. **(E)** Extracellular adenosine accumulation (nM) measured by HPLC in U87MG GSCs siRNA-HIF-1α, siRNA-HIF-2α, and siRNA-Mix under hypoxia for 24 h. **(F)** Representative western blot (left panel) of CD73, PAP, and β-actin in U87MG-GSCs knock down (siRNA) for CD73, PAP, and CD73/PAP (siRNA-Mix) under hypoxia for 24 h. **(G)** Extracellular adenosine accumulation (nM) measured by HPLC in U87MG-GSCs siRNA-CD73, siRNA-PAP, and siRNA-Mix under hypoxia for 24 h. Adenosine concentrations in A, E and G were normalized to the total protein levels (μg) in each condition. siRNA-scramble was used as a negative control of transfection in D-G. Graphs represent the mean ± S.D. $^{*}P \leq 0.05$; $^{**}P \leq 0.01$; $^{***}P \leq 0.001$ normoxia versus hypoxia (A–C) or siRNA scramble under normoxia versus other conditions (E and G); $\#P < 0.05$; $\#\#P < 0.01$ siRNA scramble under hypoxia versus other conditions (E and G). $\#P < 0.05$ U87MG versus PC (A). $n = 3$ (three independent experiments performed in duplicate).

2.15. Immunohistofluorescence

Subcutaneous tumor samples were paraffin embedded and 5 µm sections were mounted on silanized slides. Histological preparations were dewaxed, rehydrated and immersed in citrate buffer (pH 6) for antigen retrieval. Samples were blocked with 2.5% normal horse serum blocking solution (S-2012, Vector laboratories) for 45 min and then incubated overnight with primary antibodies (Table S1) at 4 °C. The secondary antibody was Alexa-488/Alexa-567 and DAPI (300 nM; Thermo Fisher Scientific) was used as a counterstain. Finally, tumor samples were visualized using an epi-fluorescence microscope (Zeiss) and data were processed using ImageJ software (NIH).

2.16. RNA sequencing and data analysis

Total RNA of U87MG-GSCs treated with MRS1220 (10 µM; Tocris®) for 24 h under hypoxia was extracted using the commercial kit Nucleospin RNA II (Macherey-Nagel) following the instructions specified by the manufacturer. The quality of total RNA was measured with the Fragment Analyzer (Advanced Analytical Technologies), considering a RNA Quality Number (RQN) equal or superior to 8 for library preparation. The RNA-seq library was performed using the TruSeq RNA Sample Preparation Kit (Illumina) and its quantitation was performed by qPCR using the Library Quant Kit Illumina GA (KAPA) following the manufacturer's instructions. Libraries were clustered on-board and sequenced to generate 125 b PE reads using the high-throughput

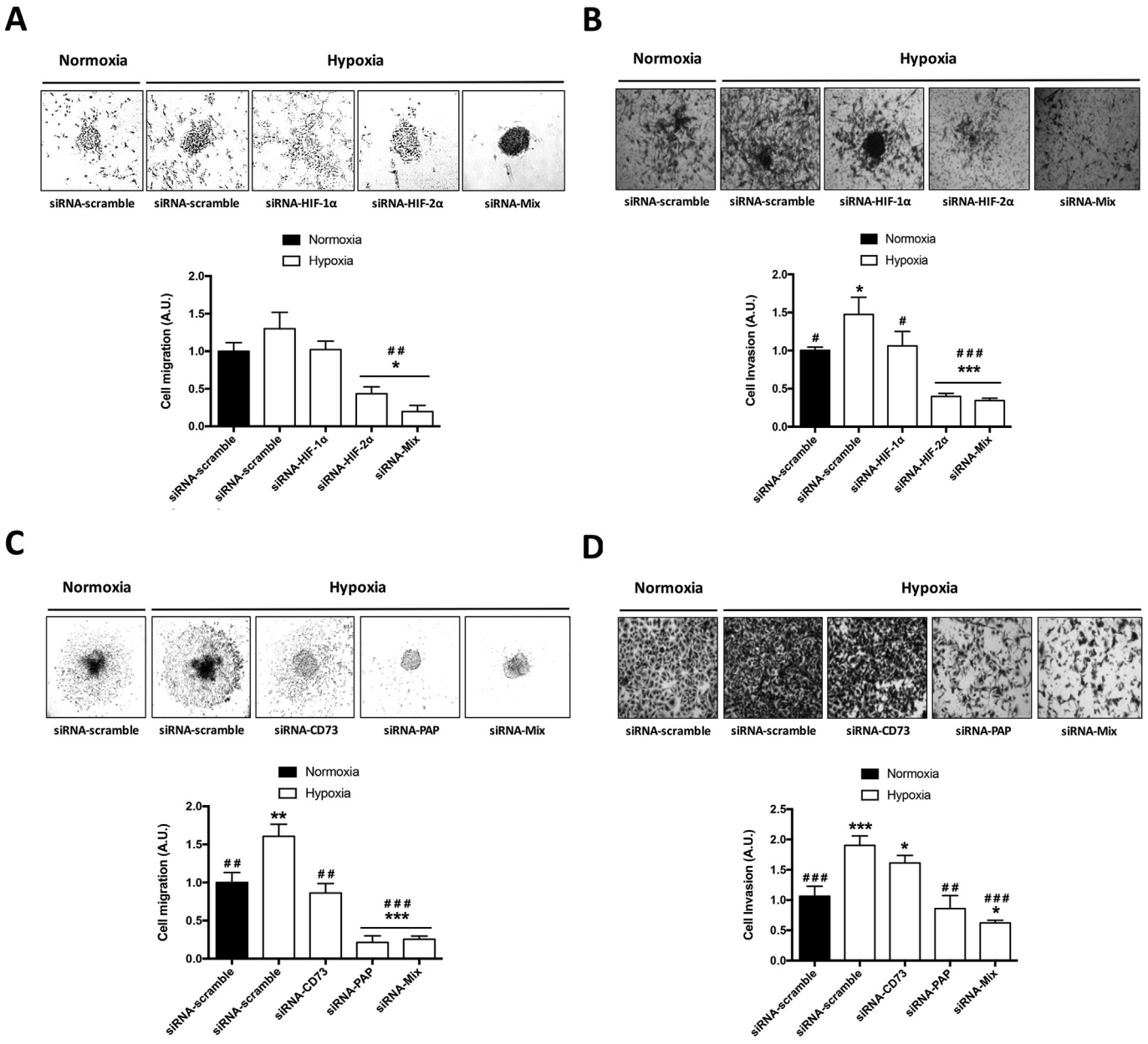

Fig. 2. Hypoxia-Inducible Factors and Ectonucleotidases control cell migration and invasion of Glioblastoma Stem-like Cells under hypoxia. (A–B) Representative images (upper panels) and quantification (lower panels) of cell migration (spreading assay) **(A)** and invasion (transwell matrigel-coated assay) **(B)** in U87MG-GSCs knock down (siRNA) for HIF-1α, HIF-2α, and HIF-1α/2α (siRNA-Mix) for 24 h under hypoxia. **(C–D)** Representative images (upper panels) and quantification (lower panels) of cell migration **(C)** and invasion **(D)** in U87MG-GSCs knock down (siRNA) for CD73, PAP, and CD73/PAP (siRNA-Mix) for 24 h under hypoxia. siRNA-scramble under normoxia was normalized to 1 (A.U. = Arbitrary Units) and used as a calibrator in A-D. Graphs represent the mean ± S.D. $*P \leq 0.05$; $**P \leq 0.01$; $***P \leq 0.001$ siRNA-scramble under normoxia versus other conditions. $\#P < 0.05$; $\#\#P < 0.01$; $\#\#P < 0.001$ siRNA scramble under hypoxia versus other conditions. Magnification in A-D = 100×. $n = 3$ (three independent experiments performed in duplicate).

sequencing system HiSeq2500 (Illumina). Sequences were mapped to the HS_GRCh38 human genome (ensembl.org) and the number of read counts per gene were determined for each library using the feature counts function of the Rsubread R library. To determine differential expression based on raw counts we used the DEseq2 R library, and a *p*-adjusted value equal or less than 0.05 was considered statistically significant, subjecting these transcripts to the Database for Annotation, Visualization and Integrated Discovery (DAVID) v6.8. Data are available on Gene Expression Omnibus (GEO) database under the following code: GSE100146.

2.17. Statistics

GraphPad Prism® 6.01 software was used to perform the statistical analysis. Values are shown as mean ± S.D., where n indicates the number of independent experiments. Statistical analysis was carried out on raw data using the Peritz F multiple means comparison test. Student's t-test was applied for unpaired data. *P* and *P*-adjusted values ≤ 0.05 were considered statistically significant.

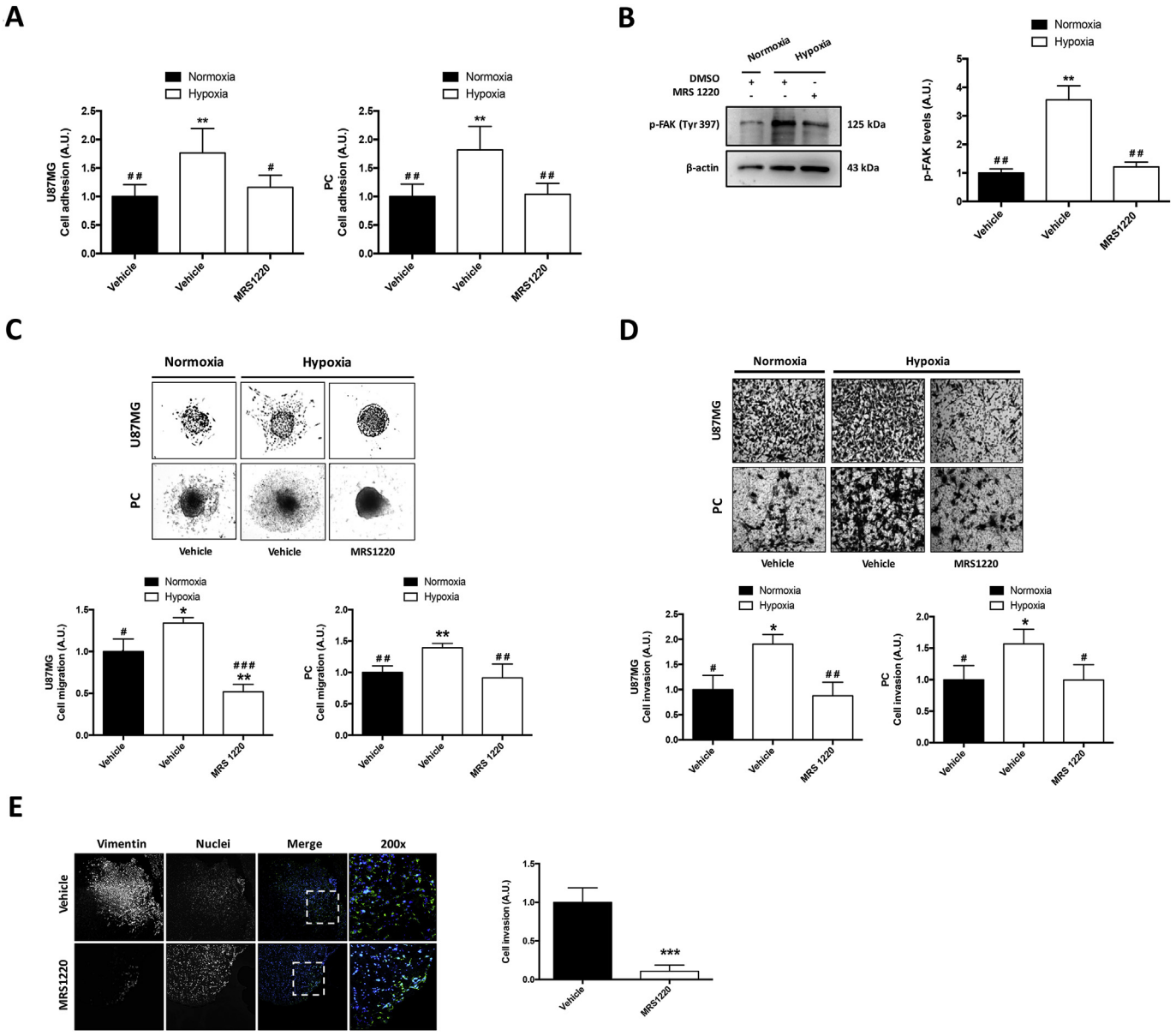

Fig. 3. The A_3 Adenosine Receptor controls cell adhesion, migration and invasion of Glioblastoma Stem-like Cells under hypoxia. (A) Cell adhesion at 2 h in U87MG (left graph) and PC (right graph) GSCs under normoxia (black box) and hypoxia (white boxes) pre-treated with vehicle or MRS1220 for 24 h. **(B)** Representative p-FAK and β-actin expression measured by western blot in U87MG-GSCs under normoxia (black box) and hypoxia (white boxes) treated with vehicle or MRS1220 for 24 h. **(C–D)** Representative images (upper panels) and quantification (lower panels) of cell migration (spreading assay) **(C)** and invasion (transwell matrigel-coated assay) **(D)** in U87MG and PC GSCs treated with vehicle or MRS1220 for 24 h under hypoxia. Magnification = 100×. **(E)** *Ex vivo* cell invasion of GSCs in organotypic mouse brain slices. GSCs were treated with vehicle and MRS1220 every 72 h during 21 days. GSCs (green) were detected inside the brain slice using a monoclonal anti-human Vimentin antibody, and DAPI (blue) was used for counterstaining nuclei. Magnification = 200×. Vehicle-treated group under normoxia was normalized to 1 (A.U. = Arbitrary Units) and used as a calibrator in A-E. Graphs represent the mean ± S.D. $*P \leq 0.05$; $**P \leq 0.01$; $***P \leq 0.001$ vehicle under normoxia versus other conditions. $\#P < 0.05$; $\#\#P < 0.01$; $\#\#P < 0.001$ vehicle under hypoxia versus other conditions. $n = 3$ (three independent experiments performed in duplicate).

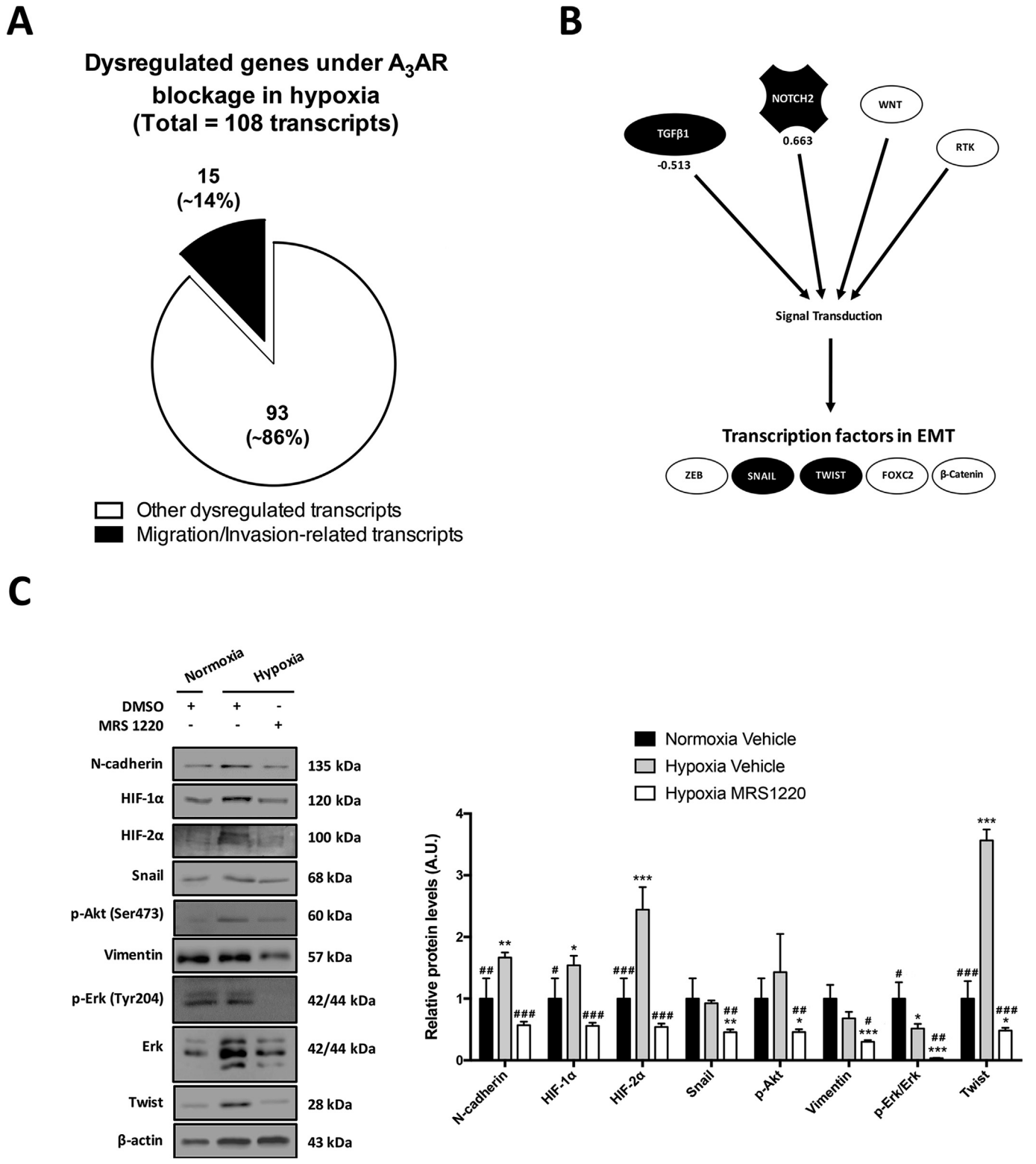

Fig. 4. A_3 Adenosine Receptor controls the expression of Epithelial-Mesenchymal Transition markers in Glioblastoma Stem-like Cells under hypoxia. (A) Pie chart of dysregulated transcripts (total = 108 transcripts) of U87MG-GSCs treated with MRS1220 for 24 h under hypoxia. Migration/Invasion-related transcripts (black) and other dysregulated transcripts (white) are presented, highlighting a total of 15 transcripts (Table 1) directly related with cell migration and invasion. **(B)** Representative diagram of dysregulated transcripts (black boxes) which control the expression of EMT transcriptional factors, SNAIL and TWIST. **(C)** Representative western blots (left panel) and quantifications (right panel) of N-cadherin, HIF-1α, HIF-2α, Snail, Vimentin, Twist, p-Erk, p-Akt, and total Erk in GSCs treated with vehicle or MRS1220 under hypoxia for 24 h. β-actin was used to normalize protein expression in C. Vehicle-treated group under normoxia was normalized to 1 (A.U. = Arbitrary Units) and used as a calibrator. Graphs represent the mean ± S.D. $*P \leq 0.05$; $**P \leq 0.01$; $***P \leq 0.001$ vehicle under normoxia versus other conditions. $\#P < 0.05$; $\#\#P < 0.01$; $\#\#P < 0.001$ vehicle under hypoxia versus other conditions. $n = 3$ (three independent experiments performed in duplicate).

Table 1
List of dysregulated transcripts directly related to cell migration and invasion processes in GSCs treated with MRS1220 under hypoxia.

ENSEMBL code	Transcripts	log2FoldChange
ENSG00000240972	macrophage migration inhibitory factor (MIF)	−0.619767062
ENSG00000144791	LIM domains containing 1 (LIMD1)	−0.606645331
ENSG00000050820	BCAR1, Cas family scaffolding protein (BCAR1)	−0.593061225
ENSG00000105329	transforming growth factor beta 1 (TGFB1)	−0.513774832
ENSG00000106211	heat shock protein family B member 1 (HSPB1)	−0.468578412
ENSG00000108518	profilin 1 (PFN1)	−0.421668514
ENSG00000118263	Kruppel like factor 7 (KLF7)	0.480616661
ENSG00000125538	interleukin 1 beta (IL1B)	0.538118636
ENSG00000187764	semaphorin 4D (SEMA4D)	0.636873292
ENSG00000116044	nuclear factor, erythroid 2 like 2 (NFE2L2)	0.661584004
ENSG00000134250	notch 2 (NOTCH2)	0.663291294
ENSG00000170961	hyaluronan synthase 2 (HAS2)	0.700113094
ENSG00000124882	epiregulin (EREG)	0.771531236
ENSG00000166923	gremlin 1, DAN family BMP antagonist (GREM1)	0.849146357
ENSG00000138061	cytochrome P450 1B member 1 (CYP1B1)	1.087534648

3. Results

3.1. Hypoxia inducible factors enhance extracellular adenosine production, increasing the expression of ectonucleotidases in Glioblastoma Stem-like Cells under hypoxia

GSCs were cultured *in vitro* under normoxia and hypoxia conditions for 24 h, the extracellular adenosine production increased 4 and 9.3 times in human GSCs obtained from the GBM U87MG cell line and PC cells, respectively under hypoxia (Fig. 1A). Similarly, mRNA (Fig. 1B) and protein (Figs. 1C and S2A) expression of A_3AR and ectonucleotidases (CD73 and PAP) increased in U87MG- and PC- GSCs under hypoxia. We evaluated the effect of HIF knock-down [HIF-1α ($KD^{HIF-1\alpha}$) and HIF-2α ($KD^{HIF-2\alpha}$)] (Fig. S2B), on the expression of ectonucleotidases and extracellular adenosine production under hypoxia. We found that CD73 and PAP expression decreased in both HIFs knock-down GSCs; however, a stronger decrease in PAP expression was observed in $KD^{HIF-2\alpha}$ GSCs (Fig. 1D), correlating with lower extracellular adenosine production under hypoxia (Figs. 1E and S2C). Because there is no difference in extracellular adenosine production between $KD^{HIF-1\alpha}$ and $KD^{HIF-2\alpha}$ GSCs (Figs. 1E and S2C), we knocked-down the expression of both CD73 (KD^{CD73}) and PAP (KD^{PAP}) and also used AOPCP as a CD73 inhibitor (Fig. 1F and Fig. S2B) accordingly to determine which ectonucleotidase is responsible for extracellular adenosine production under hypoxia. We found that knock-down of both ectonucleotidases decreased extracellular adenosine production under hypoxia, however the effect was stronger in KD^{PAP} GSCs and when both ectonucleotidases were knocked-down (Figs. 1G and S2D).

3.2. HIF-2 and prostatic acid phosphatase expression increases the cell migration and invasion of Glioblastoma Stem-like Cells under hypoxia

GSCs of the U87MG cell line (Fig. 2) and PC cells (Fig. S3) had higher cell migration/invasion under hypoxia than normoxia. Cell migration/invasion decreased with both HIF knock-down (Figs. 2A–B and S3A) in the U87MG cell line (Fig. 2A and B) and PC cells (Fig. S3A). However, a stronger effect was observed in $KD^{HIF-2\alpha}$ U87MG-GSCs, decreasing cell migration and invasion by ~68% and ~72%, respectively (Fig. 2A and B). Due to the relationship between the expression of HIFs and extracellular adenosine production we decided to evaluate the effect of ectonucleotidase expression on cell migration/invasion; showing decreased cell migration in U87MG- (Fig. 2C) and PC- (Fig. S3B) GSCs with both ectonucleotidases knocked-down, although the effect in KD^{PAP} was stronger than KD^{CD73} GSCs under hypoxia (Figs. 2C and S3B). Cell invasion was only decreased in KD^{PAP} GSCs (Figs. 2D and S3B). All together, these results ratify the importance of PAP-mediated adenosine production in GSCs under hypoxia conditions, suggesting a remarkable role of PAP in the hypoxic niche of GBM.

3.3. A_3AR blockade decreases cell adhesion and cell migration/invasion of Glioblastoma Stem-like Cells under hypoxia

To determine the contribution of the A_3AR to cell adhesion and migration/invasion of GSCs we used MRS1220, a selective antagonist of this receptor [18]. We found that A_3AR blockade decreased cell adhesion in U87MG-GSCs and PC-GSCs by ~32% and ~22%, respectively (Fig. 3A). To evaluate the effect of MRS1220 on focal adhesions, we evaluated the protein content of phospho-Focal Adhesion Kinase (p-FAK). We observed a decrease in p-FAK content in U87MG-GSCs treated with MRS1220 (Fig. 3B). Moreover, A_3AR blockade decreased cell migration ~0.61 and ~0.35 times in U87MG- and PC- GSCs, respectively (Fig. 3C). Similarly, cell invasion decreased when using the selective A_3AR antagonist, ~0.65 and ~0.36 in U87MG- and PC- GSCs, respectively (Fig. 3D). An *ex vivo* brain slice model was used to evaluate the invasiveness of GSCs and treated with the selective A_3AR antagonist. MRS1220 decreased cell invasion by ~89%, compared to the vehicle treated group (Fig. 3E).

3.4. A_3AR blockade decreases the expression of EMT markers in GSCs under hypoxic conditions

We evaluated the transcriptome profile of GSCs treated with MRS1220 under hypoxia during 24 h using the RNAseq technique. The analysis showed that 108 (~1%) of 10,010 sequenced transcripts were dysregulated by MRS1220 treatment and 15 of these transcripts were directly related with migration and invasion processes (Fig. 4A and Table 1). A signaling pathway analysis shows that TWIST and SNAIL may be regulated by the A_3AR (Fig. 4B). To confirm these results, we evaluated HIFs (HIF-1α and HIF-2α), Twist, Snail, N-cadherin and Vimentin protein levels in GSCs treated with MRS1220 under hypoxia. Expression of HIFs, Twist and N-cadherin increased under hypoxia (Fig. 4C). The A_3AR blockade decreased this overexpression and also attenuated Snail and Vimentin levels (Fig. 4C and Fig. S4A). These results were confirmed *in vivo* with GBM subcutaneous tumor samples derived from human GSCs in a murine model under MRS1220 treatment analyzed by immunofluorescence, showing a decrease in Twist and Snail, and up-regulation of E-cadherin (Fig. S4B). Finally, Erk protein levels increased under hypoxia and the use of MRS1220 reduces this increase and also decreases Akt and Erk phosphorylation (Fig. 4C).

4. Discussion

4.1. Hypoxia and extracellular adenosine in GSCs

We previously reported that extracellular adenosine levels were increased in GSCs compared to non-GSCs [18], and increase even more under hypoxia conditions [26], however, adenosine production by CD73 and PAP had not yet been described in GSCs under hypoxia. In this work, we showed that GSCs exposed to hypoxia produce higher levels of extracellular adenosine compared to normoxia conditions. In addition, these cells also increased the levels of both their adenosine-producing enzymes, CD73 and PAP. We showed that the expression of CD73 and PAP decreased in GSCs-$KD^{HIF-1\alpha}$ and GSCs-$KD^{HIF-2\alpha}$. Our results suggest that HIF-1α and HIF-2α regulate the expression of CD73 and PAP; however, the effect of HIF-2α, which is related with chronic hypoxia [30,31], appears to be stronger on the regulation of PAP levels, which in part had already been confirmed by other authors [19]. All

these results suggest that CD73 is involved in the synthesis of extracellular adenosine in early stages of hypoxia, whereas PAP would have a role in chronic hypoxia, an important feature of hypoxic niches where GSCs reside [17]. This indicates that the production of extracellular adenosine can be compensated at different degrees of hypoxia, emphasizing that its levels may be increased even in chronic hypoxic niches (see Fig. 5).

4.2. Extracellular adenosine production in GSCs invasion

Previously EMT and invasive potential of GSCs had been described [32–36], however the role of extracellular adenosine production in GSCs invasion had not been studied. In this study we demonstrate that the decrease in extracellular adenosine production with GSCs-KD^{CD73} and GSCs-KD^{PAP} downregulated cell migration potential under hypoxia, with a greater effect observed in the PAP knock-down condition, suggesting a fundamental role of the activity of this enzyme in the production of extracellular adenosine in GSCs. Interestingly, only GSCs-KD^{PAP} decrease invasion potential, ratifying the specific importance of this ectonucleotidase in hypoxia, indicating that PAP would be more important than CD73 in stages of chronic hypoxia, while being mainly regulated by HIF-2α [19,31]. In their study, Liu *et al.*, state that A_{2B}AR would be the receptor involved in the HIF-2α-dependent-PAP activity, however a role of A_3AR is not ruled out. Although A_{2B}AR and A_3AR activate different signaling pathways, some of them also converge, such as PI3K and ERK [18,19], so they could have a synergic or complementary effect in the activation of these pathways, thereby promoting the stabilization of HIF-2α and the production of extracellular adenosine mediated by PAP in chronic hypoxia [19]. Adenosine could also activate A_1 and A_{2A} receptors, however these are classified as high affinity receptors that activate at mM adenosine concentrations, and it has been reported that the major effects of adenosine in μM

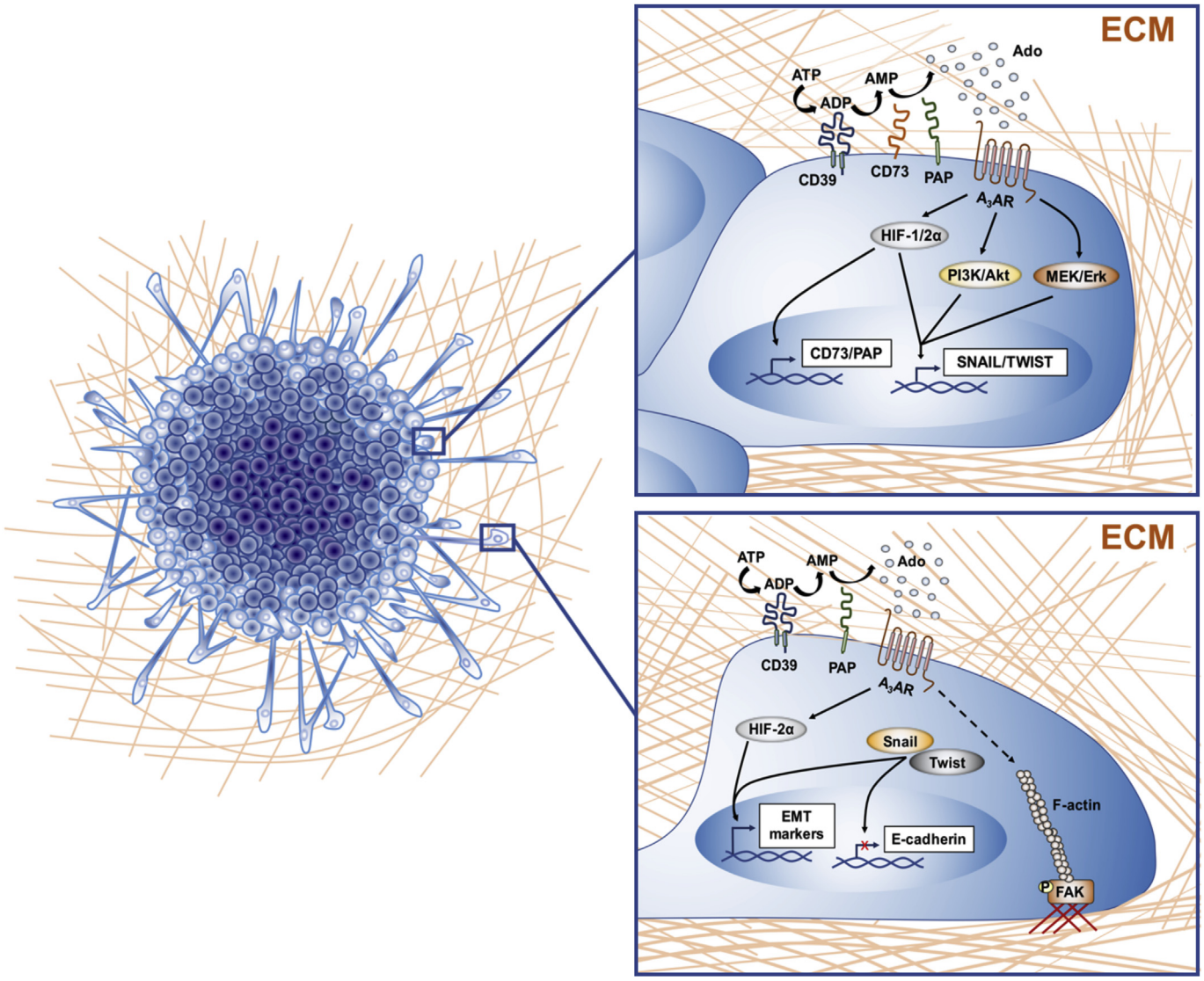

Fig. 5. Extracellular adenosine through A_3AR activation controls the Epithelial-Mesenchymal Transition and cell migration/invasion of Glioblastoma Stem-like Cells under hypoxia. During early stages of hypoxia (upper right panel), the extracellular adenosine production increases due to the increased expression of both ectonucleotidases, CD73, and PAP. This extracellular adenosine activates its low affinity receptor A_3AR which by signaling downstream to HIF-1α and HIF-2α regulate the expression of both ectonucleotidases, CD73, and PAP, generating a positive loop of extracellular adenosine generation. The activation of the A_3AR promotes the expression of EMT transcriptional factors SNAIL and TWIST through the activation of HIFs, PI3K/Akt, and MEK/Erk signaling pathways. At a later stage (lower right panel), extracellular adenosine under hypoxia is generated mainly by PAP activity, maintaining A_3AR activation which regulates GSCs adhesion with the ECM through the activation of FAK. A_3AR, through the transcriptional factors Snail and Twist, negatively regulates the expression of E-cadherin, promoting the switch to N-cadherin. Moreover, A_3AR activation provides downstream regulation, through HIF-2α and together with Snail/Twist, of the expression of EMT markers and, therefore, promotes cell migration and invasion of GSCs under hypoxia.

concentrations act through its low affinity receptors, A_{2B}AR and A_3AR [37]. It would also be interesting to study the role of low affinity receptors in this pathology, in conditions where adenosine is aberrantly increased, as tumor cells and GSCs under hypoxia conditions where its production and levels are further exacerbated [7] and HIFs stabilization is promoted [31]. In addition, samples from GBM patients showed that low affinity adenosine receptors are the most expressed, which confirms its importance in this study, although this does not rule out that high affinity receptors could have an effect [7,16,37]. In summary, our results suggest that HIFs expression promote cell migration/invasion of GSCs under hypoxia by regulating CD73 and/or PAP expression and subsequent extracellular adenosine production.

Previously our research group demonstrated that the A_3AR regulates GSCs chemoresistance through the PI3K/Akt and MEK/ERK pathways [18], however their role in cell adhesion, migration, and invasion had not yet been described in GSCs. These signaling pathways have been involved in the expression of transcription factors that regulate cell migration/invasion in malignant glioma, such as Twist and Snail [38]. In turn, these transcription factors have been involved in the induction of morphological changes in GBM cells, favoring the acquisition of a more invasive phenotype [39,40]. Also, it has been reported that under hypoxia the expression of FAK protein is increased, favoring cell adhesion processes in GBM [41]. This is very relevant since chemoresistance together with cell invasion are the main cause of GBM relapses, ratifying the importance of studying the mechanisms that lead to invasion, such as cell adhesion and migration. Proteins involved in the formation of focal adhesions and cell migration had already been described for GBM cellular models, but not for GSCs [42,43]. In this study we demonstrated that the A_3AR is involved in the cell adhesion of GSCs, through the activation of FAK (p-FAK). It had been shown that caffeine was able to decrease the migration of GBM cells through the negative regulation of FAK activation [44], but the role of extracellular adenosine in the regulation of these proteins had not yet been described for GSCs under hypoxia conditions. During hypoxic conditions the level of extracellular adenosine is elevated, therefore, it is possible that the activation of adenosine receptors can modulate the expression and/or activity of FAK in GSCs under hypoxia. Several studies have demonstrated that the regulation of these proteins, together with regular adhesion, are involved in migratory processes and in many cases with invasive capacity in different types of cancer, including GBM [45,46]. In this study it was also shown that A_3AR blockade decreased cell migration/invasion of GSCs in hypoxia, which is consistent with that observed in non-GSCs [47].

4.3. Adenosine-dependent pathways in GSCs invasion

It had previously been described that the PI3K/Akt pathway may participate in promoting GSCs invasion [36], however it is not clear if the role of extracellular adenosine and the A_3AR in GSCs invasion acts through this signaling pathway. In this context, our previous results obtained for chemoresistance suggest that, through activation of A_3AR, the PI3K/Akt and MEK/Erk pathways could be involved in other characteristics of GSCs tumor progression, such as EMT, cell migration and invasion, although we still need to understand the mechanisms and signaling pathways involved in these processes [7,18]. Previously, we showed that A_3AR activation does not only promote mechanisms of chemoresistance [18] but also the expression of endothelial markers [26]. This indicates that the A_3AR could be an important master regulator of all these processes, however, this does not mean that A_3AR signaling affects all cells, since in the GSCs culture plate different “pools” or cell subpopulations that activate A_3AR could co-exist, but each one generates independent signaling. In addition, we do not discard the participation of A_{2B}AR which is also a low affinity adenosine receptor that could be activated during hypoxia thereby regulating cell invasion, angiogenesis, and/or chemoresistance [7].

Erk plays an important role, because phosphorylation of Paxillin by Erk promotes disassembly of focal adhesions, favoring cell motility and migration [46]. Although these signaling pathways are still under study, an important result that helps to understand this mechanism is the RNAseq data obtained in GSCs treated with MRS1220 under hypoxia, which shows several genes involved, not only in cell migration, and invasion, but also in tumor progression. For example, treatment with MRS1220 under hypoxia decreases the expression of the macrophage migration inhibitory factor (MIF), which is an oncogene associated with poor prognosis for several cancers including GBM [48,49]. For this reason, it would be interesting to further study the signaling pathways and target genes regulated by adenosine and its receptors. In this context, we wanted to study whether A_3AR is involved in EMT, cell migration, and invasion processes under hypoxia, and how HIFs might play a role [50,51]. As expected, HIF-1α and HIF-2α increased their protein levels in hypoxia, which was prevented by A_3AR blockade, proposing extracellular adenosine as a regulator of the expression and/or stability of these factors, even under hypoxia, where these factors are known to be aberrantly elevated. In addition, the blockade of A_3AR under hypoxia decreases the levels of EMT markers, suggesting that this receptor is involved in EMT, cell migration, and invasion. As a projection, we propose an eventual therapy targeting the extracellular adenosine axis, which would not only affect the cells that surround the tumor, but also GSCs in the hypoxic niches, that are responsible for the progression and recurrence of GBM.

Declarations of interest

None.

Funding

This study was supported by grants from Fondo Nacional de Desarrollo Científico y Tecnológico (FONDECYT No 1160777 to C.Q; No 3180749 to A.T.; No 3180621 to I.N.); from Comisión Nacional de Investigación Científica y Tecnológica (CONICYT No 21131009 to A.T.; No 21181983 to J.I.E.); and Vicerrectoría de Investigación, Desarrollo y Creación Artística (VIDCA) from Universidad Austral de Chile to A.T.

Acknowledgements

Orlando Contreras-López and Tomás Moyano at Pontificia Universidad Católica de Chile who performed and supervised RNAseq experiments and data analysis. Thanks to John James Finnolli for his help in proofreading and editing.

Appendix ASupplementary data

Supplementary data to this article can be found online at https://doi.org/10.1016/j.canlet.2019.01.004.

References

[1] Q.T. Ostrom, H. Gittleman, J. Fulop, M. Liu, R. Blanda, C. Kromer, Y. Wolinsky, C. Kruchko, J.S. Barnholtz-Sloan, CBTRUS statistical report: primary brain and central nervous system tumors diagnosed in the United States in 2008-2012, Neuro Oncol. (2012) 1–62.
[2] Y.P. Ramirez, J.L. Weatherbee, R.T. Wheelhouse, A.H. Ross, Glioblastoma multiforme therapy and mechanisms of resistance, Pharmaceuticals (2013) 1475–1506.
[3] Á.S. Torres, J.I. Erices, D.A. Uribe, et al., Current therapeutic alternatives and new perspectives in glioblastoma multiforme, Curr. Med. Chem. (2017) 2781–2795.
[4] B. Ortensi, M. Setti, D. Osti, G. Pelicci, Cancer stem cell contribution to glioblastoma invasiveness, Stem Cell Res. Ther. (2013) 18–29.
[5] S. Asuthkar, K.K. Velpula, C. Chetty, B. Gorantla, J.S. Rao, Epigenetic regulation of miRNA-211 by MMP-9 governs glioma cell apoptosis, chemosensitivity and radiosensitivity, Oncotarget (2012) 1439–1454.
[6] F. Chen, X. Zhuang, L. Lin, P. Yu, Y. Wang, Y. Shi, G. Hu, Y. Sun, New horizons in tumor microenvironment biology: challenges and opportunities, BMC Med. (2015) 45–59.
[7] D. Uribe, Á. Torres, J.D. Rocha, I. Niechi, C. Oyarzún, L. Sobrevia, R. San Martín, C. Quezada, Multidrug resistance in glioblastoma stem-like cells: role of the hypoxic

microenvironment and adenosine signaling, Mol. Aspect. Med. (2017) 140–151.
[8] L. Yang, C. Lin, L. Wang, H. Guo, X. Wang, Hypoxia and hypoxia-inducible factors in glioblastoma multiforme progression and therapeutic implications, Exp. Cell Res. (2012) 2417–2426.
[9] O. Méndez, J. Zavadil, M. Esencay, Y. Lukyanov, D. Santovasi, S.C. Wang, E.W. Newcomb, D. Zagzag, Knock down of HIF-1alpha in glioma cells reduces migration in vitro and invasion in vivo and impairs their ability to form tumor spheres, Mol. Canc. (2010) 133–144.
[10] S.W. Crowder, D.A. Balikov, Y.S. Hwang, H.J. Sung, Cancer stem cells under hypoxia as a chemoresistance factor in breast and brain, Curr. Pathobiol. Rep. (2014) 33–40.
[11] M. Tafani, M. Di Vito, A. Frati, L. Pellegrini, E. De Santis, G. Sette, A. Eramo, P. Sale, E. Mari, A. Santoro, A. Raco, M. Salvati, R. De Maria, M.A. Russo, Pro-inflammatory gene expression in solid glioblastoma microenvironment and in hypoxic stem cells from human glioblastoma, J. Neuroinflammation (2011) 32–48.
[12] F. Nigim, J. Cavanaugh, A.P. Patel, W.T. Curry Jr., S. Esaki, E.M. Kasper, A.S. Chi, D.N. Louis, R.L. Martuza, S.D. Rabkin, H. Wakimoto, Targeting hypoxia-inducible factor 1α in a new orthotopic model of glioblastoma recapitulating the hypoxic tumor microenvironment, J. Neuropathol. Exp. Neurol. (2015) 710–722.
[13] L. Zhang, G. Huang, X. Li, Y. Zhang, Y. Jiang, J. Shen, J. Liu, Q. Wang, J. Zhu, X. Feng, J. Dong, C. Qian, Hypoxia induces epithelial-mesenchymal transition via activation of SNAI1 by hypoxia-inducible factor -1α in hepatocellular carcinoma, BMC Canc. (2013) 108–117.
[14] J. Zuo, J. Wen, M. Lei, M. Wen, S. Li, X. Lv, Z. Luo, G. Wen, Hypoxia promotes the invasion and metastasis of laryngeal cancer cells via EMT, Med. Oncol. (2016) 15–24.
[15] T. Takahashi, K. Otsuguro, T. Ohta, S. Ito, Adenosine and inosine release during hypoxia in the isolated spinal cord of neonatal rats, Br. J. Pharmacol. (2010) 1806–1816.
[16] C. Quezada, W. Garrido, C. Oyarzún, K. Fernández, R. Segura, R. Melo, P. Casanello, L. Sobrevia, R. San Martín, 5'-ectonucleotidase mediates multiple-drug resistance in glioblastoma multiforme cells, J. Cell. Physiol. (2013) 602–608.
[17] W. Garrido, J.D. Rocha, C. Jaramillo, K. Fernandez, C. Oyarzun, R. San Martin, C. Quezada, Chemoresistance in high-grade gliomas: relevance of adenosine signalling in stem-like cells of glioblastoma multiforme, Curr. Drug Targets (2014) 931–942.
[18] A. Torres, Y. Vargas, D. Uribe, C. Jaramillo, A. Gleisner, F. Salazar-Onfray, M.N. López, R. Melo, C. Oyarzún, R. San Martín, C. Quezada, Adenosine A3 receptor elicits chemoresistance mediated by multiple resistance-associated protein-1 in human glioblastoma stem-like cells, Oncotarget (2016) 67373–67386.
[19] T.Z. Liu, X. Wang, Y.F. Bai, H.Z. Liao, S.C. Qiu, Y.Q. Yang, X.H. Yan, J. Chen, H.B. Guo, S.Z. Zhang, The HIF-2alpha dependent induction of PAP and adenosine synthesis regulates glioblastoma stem cell function through the A2B adenosine receptor, Int. J. Biochem. Cell Biol. (2014) 8–16.
[20] A.R. Cappellari, L. Rockenbach, F. Dietrich, V. Clarimundo, T. Glaser, E. Braganhol, A.L. Abujamra, R. Roesler, H. Ulrich, A.M. Battastini, Characterization of ectonucleotidases in human medulloblastoma cell lines: ecto-5'NT/CD73 in metastasis as potential prognostic factor, PLoS One (2012) e47468.
[21] Z.H. Ren, C.Z. Lin, W. Cao, R. Yang, W. Lu, Z.Q. Liu, Y.M. Chen, X. Yang, Z. Tian, L.Z. Wang, J. Li, X. Wang, W.T. Chen, T. Ji, C.P. Zhang, CD73 is associated with poor prognosis in HNSCC, Oncotarget (2016) 61690–61702.
[22] J. Stagg, U. Divisekera, H. Duret, T. Sparwasser, M.W. Teng, P.K. Darcy, M.J. Smyth, CD73-deficient mice have increased antitumor immunity and are resistant to experimental metastasis, Cancer Res. (2011) 2892–2900.
[23] X. Zhi, S. Chen, P. Zhou, Z. Shao, L. Wang, Z. Ou, L. Yin, RNA interference of ecto-5'-nucleotidase (CD73) inhibits human breast cancer cell growth and invasion, Clin. Exp. Metastasis (2007) 439–448.
[24] J. Stagg, U. Divisekera, N. McLaughlin, J. Sharkey, S. Pommey, D. Denoyer, K.M. Dwyer, M.J. Smyth, Anti-CD73 antibody therapy inhibits breast tumor growth and metastasis, Proc. Natl. Acad. Sci. U. S. A. (2010) 1547–1552.
[25] A.R. Cappellari, G.J. Vasques, L. Bavaresco, E. Braganhol, A.M. Battastini, Involvement of ecto-5'-nucleotidase/CD73 in U138MG glioma cell adhesion, Mol. Cell. Biochem. (2012) 315–322.
[26] R. Rocha, Á. Torres, K. Ojeda, D. Uribe, D. Rocha, J. Erices, I. Niechi, P. Ehrenfeld, R. San Martín, C. Quezada, The adenosine A_3 receptor regulates differentiation of glioblastoma stem-like cells to endothelial cells under hypoxia, Int. J. Mol. Sci. 18 (2018) 19(4).
[27] P. Vaupel, A. Mayer, Hypoxia-driven adenosine accumulation: a crucial microenvironmental factor promoting tumor progression, Adv. Exp. Med. Biol. (2016) 177–183.
[28] V.R. Dasari, K. Kaur, K.K. Velpula, M. Gujrati, D. Fassett, J.D. Klopfenstein, D.H. Dinh, J.S. Rao, Upregulation of PTEN in glioma cells by cord blood mesenchymal stem cells inhibits migration via downregulation of the PI3K/Akt pathway, PLoS One (2010) 10350–10362.
[29] H. Kim, E. Kim, M. Park, E. Lee, K. Namkoong, Organotypic hippocampal slice culture from the adult mouse brain: a versatile tool for translational neuropsychopharmacology, Prog. Neuro-Psychopharmacol. Biol. Psychiatry (2013) 36–43.
[30] M. Bhagat, J.K. Palanichamy, P. Ramalingam, M. Mudassir, K. Irshad, K. Chosdol, C. Sarkar, P. Seth, S. Goswami, S. Sinha, P. Chattopadhyay, HIF-2α mediates a marked increase in migration and stemness characteristics in a subset of glioma cells under hypoxia by activating an Oct-4/Sox-2-Mena (INV) axis, Int. J. Biochem. Cell Biol. (2016) 60–71.
[31] Q. Lin, X. Cong, Z. Yun, Differential hypoxic regulation of hypoxia-inducible factors 1alpha and 2alpha, Mol. Canc. Res. 9 (6) (2011) 757–765.
[32] Y. Iwadate, Epithelial-mesenchymal transition in glioblastoma progression, Oncol. Lett. (2016) 1615–1620.
[33] C. Kubelt, K. Hattermann, S. Sebens, H.M. Mehdorn, J. Held-Feindt, Epithelial-to-mesenchymal transition in paired human primary and recurrent glioblastomas, Int. J. Oncol. (2015) 2515–2525.
[34] R. Laczko, K.M. Szauter, M.K. Jansen, P. Hollosi, M. Muranyi, J. Molnar, K.S. Fong, A. Hinek, K. Csiszar, Active lysyl oxidase (LOX) correlates with focal adhesion kinase (FAK)/paxillin activation and migration in invasive astrocytes, Neuropathol. Appl. Neurobiol. (2007) 631–643.
[35] J.K. Myung, S.A. Choi, S.K. Kim, K.C. Wang, S.H. Park, Snail plays an oncogenic role in glioblastoma by promoting epithelial mesenchymal transition, Int. J. Clin. Exp. Pathol. (2014) 1977–1987.
[36] Y. Jiao, H. Li, Y. Liu, A. Guo, X. Xu, X. Qu, S. Wang, J. Zhao, Y. Li, Y. Cao, Resveratrol inhibits the invasion of glioblastoma-initiating cells via down-regulation of the PI3K/Akt/NF-κB signaling pathway, Nutrients (2015) 4383–4402.
[37] B.B. Fredholm, Adenosine–a physiological or pathophysiological agent? J. Mol. Med. (Berl.) (2014) 201–206.
[38] R. Mahabir, M. Tanino, A. Elmansuri, L. Wang, T. Kimura, T. Itoh, Y. Ohba, H. Nishihara, H. Shirato, M. Tsuda, S. Tanaka, Sustained elevation of Snail promotes glial-mesenchymal transition after irradiation in malignant glioma, Neuro Oncol. (2014) 671–685.
[39] J.V. Joseph, S. Conroy, K. Pavlov, P. Sontakke, T. Tomar, E. Eggens-Meijer, V. Balasubramaniyan, M. Wagemakers, W.F. den Dunnen, F.A. Kruyt, Hypoxia enhances migration and invasion in glioblastoma by promoting a mesenchymal shift mediated by the HIF1α-ZEB1 axis, Cancer Lett. (2015) 107–116.
[40] W. Xu, Z. Yang, N. Lu, A new role for the PI3K/Akt signaling pathway in the epithelial-mesenchymal transition, Cell Adhes. Migrat. (2015) 317–324.
[41] C.S. Xu, Z.F. Wang, X.D. Huang, L.M. Dai, C.J. Cao, Z.Q. Li, Involvement of ROS-alpha v beta 3 integrin-FAK/Pyk2 in the inhibitory effect of melatonin on U251 glioma cell migration and invasion under hypoxia, J. Transl. Med. (2015) 95–107.
[42] L.H. Sun, F.Q. Yang, C.B. Zhang, Y.P. Wu, J.S. Liang, S. Jin, Z. Wang, H.J. Wang, Z.S. Bao, Z.X. Yang, T. Jiang, Overexpression of paxillin correlates with tumor progression and predicts poor survival in glioblastoma, CNS Neurosci. Ther. (2017) 69–75.
[43] M. Natarajan, T.P. Hecker, C.L. Gladson, FAK signaling in anaplastic astrocytoma and glioblastoma tumors, Cancer J. (2003) 126–133.
[44] Y. Chen, W.C. Chou, Y.M. Ding, Y.C. Wu, Caffeine inhibits migration in glioma cells through the ROCK-FAK pathway, Cell. Physiol. Biochem. (2014) 1888–1898.
[45] J. Cha, S.G. Kang, P. Kim, Strategies of mesenchymal invasion of patient-derived brain tumors: microenvironmental adaptation, Sci. Rep. (2016) e24912.
[46] A.M. López-Colomé, I. Lee-Rivera, R. Benavides-Hidalgo, E. López, Paxillin: a crossroad in pathological cell migration, J. Hematol. Oncol. (2017) 50–65.
[47] S. Gessi, V. Sacchetto, E. Fogli, S. Merighi, K. Varani, P.G. Baraldi, M.A. Tabrizi, E. Leung, S. Maclennan, P.A. Borea, Modulation of metalloproteinase-9 in U87MG glioblastoma cells by A3 adenosine receptors, Biochem. Pharmacol. (2010) 1483–1495.
[48] Z. Wang, Y. Xue, P. Wang, J. Zhu, J. Ma, MiR-608 inhibits the migration and invasion of glioma stem cells by targeting macrophage migration inhibitory factor, Oncol. Rep. (2016) 2733–2742.
[49] Y. Tang, W. Wan, L. Wang, S. Ji, J. Zhang, microRNA-451 inhibited cell proliferation, migration and invasion through regulation of MIF in renal cell carcinoma, Int. J. Clin. Exp. Pathol. (2015) 15611–15621.
[50] W. Wu, Q. Hu, E. Nie, T. Yu, Y. Wu, T. Zhi, K. Jiang, F. Shen, Y.1 Wang, J.1 Zhang, Y. You, Hypoxia induces H19 expression through direct and indirect Hif-1α activity, promoting oncogenic effects in glioblastoma, Sci. Rep. (2017) 45029–45042.
[51] M. Mimeault, S.K. Batra, Hypoxia-inducing factors as master regulators of stemness properties and altered metabolism of cancer- and metastasis-initiating cells, J. Cell Mol. Med. (2013) 30–54.